



Optical gain at 1.55 μm of $\text{Er}(\text{TMHD})_3$ complex doped polymer waveguides based on the intramolecular energy transfer effect

JIYUN ZHU, BAOPING ZHANG, YUYANG HUANG, ZIYUE LV, LEIYING YING, YANG MEI,  ZHIWEI ZHENG, AND DAN ZHANG* 

School of Electronic Science and Engineering (National Model Microelectronics College), Xiamen University, Xiamen 361005, China

*zhangdan@xmu.edu.cn

Abstract: Based on the intramolecular energy transfer mechanism between organic ligand TMHD (2, 2, 6, 6-tetramethyl-3, 5-heptanedione) and central Er^{3+} ions, optical gains at 1.55 μm were demonstrated in three structures of polymer waveguides using complex $\text{Er}(\text{TMHD})_3$ -doped polymethylmethacrylate (PMMA) as the active material. With the excitation of two low-power UV light-emitting diodes (LEDs) instead of 980 or 1480 nm lasers, relative gains of 3.5 and 4.1 dB cm^{-1} were achieved in a 1-cm-long rectangular waveguide with an active core of $\text{Er}(\text{TMHD})_3$ -doped PMMA polymer. Meanwhile, relative gain of 3.0 dB cm^{-1} was obtained in an evanescent-field waveguide with cross-section of $4 \times 4 \mu\text{m}^2$ using passive SU-8 polymer as core and a $\sim 1\text{-}\mu\text{m}$ -thick $\text{Er}(\text{TMHD})_3$ -doped PMMA as upper cladding. By growing a 100 nm thick aluminum mirror and active lower cladding, the optical gain was doubled to 6.7 dB cm^{-1} in evanescent-field waveguides because of the stimulated excitation of Er^{3+} ions in the upper and lower cladding and the improved absorption efficiency.

© 2023 Optica Publishing Group under the terms of the [Optica Open Access Publishing Agreement](#)

1. Introduction

With the successful application of erbium-doped fiber amplifiers (EDFAs) in long-distance optical fiber communication in the C-band (1530–1565 nm), erbium-doped waveguide amplifiers (EDWAs), which are suitable for integrating photonic chips, have attracted extensive attention in the past two decades. EDWAs can be integrated with active or passive optical devices, such as Mach–Zehnder interferometers (MZI), arrayed waveguide gratings (AWG), and micro-ring resonators (MRR), to compensate for the 1.55 μm optical loss in an efficient on-chip optical system [1–5]. Erbium-doped inorganic materials [6–8] (e.g., silicate, phosphate, crystals, and alumina) or organic materials (e.g., organic complexes or oleic acid-modified nanoparticles) can be used to fabricate EDWAs. Recently, an optical gain of 3.6 dB cm^{-1} at 1.53 μm was obtained in an Er:LNOI waveguide pumped by a 980 nm semiconductor laser with a pump power of 21 mW [9]. An on-chip net gain of 1.43 dB cm^{-1} at 1.55 μm in an Er:Si₃N₄ waveguide was achieved under the excitation of a 1480 nm laser with a 245 mW pump power [10]. Compared with the above inorganic materials, polymers have the advantages of simple processing methods, low cost, easy adjustment of the refractive index, and compatibility with various substrates. The dissolution of inorganic erbium salts in polymers could be solved by encapsulating Er^{3+} ions into organic complexes or oleic acid-modified nanoparticles, such as $\text{Er}(\text{DBM})_3\text{phen}$, $\text{Er}(\text{TTA})_3(\text{TPPO})_2$, $\text{LaF}_3: \text{Er}^{3+}, \text{Yb}^{3+}$, and $\text{NaYF}_4: \text{Er}^{3+}, \text{Yb}^{3+}$ nanoparticles [11]. Poly(methyl methacrylate) (PMMA), polystyrene (PS), and polycarbonate (PC) are used as doped hosts for these complexes and nanoparticles to fabricate polymer EDWAs [12–14]. Currently, Er^{3+} , Yb^{3+} codoped nanoparticles have become the mainstream materials for preparing polymer EDWAs because of their advantages of low phonon energy and the typical gain value was 6.2 dB cm^{-1} under the excitation of a 270 mW 980 nm laser [15]. Although Er^{III} complexes were proposed

as early as 1997, only a few reports have been published to date [16–19]. These shortcomings include a small absorption cross-section at 980 nm, low metastable life of Er^{3+} ions, and inability to withstand excessive pump laser power, limiting the application and development of Er^{III} complexes in polymer EDWAs. For both inorganic and organic EDWAs, commercial 980 nm or 1480 nm semiconductor lasers are often selected as the pump sources to realize stimulated radiation of Er^{3+} ions because of the alignment of the narrow absorption spectrum of the lasers and Er^{3+} ions. However, high commercialization costs and the high laser pump energy would lead to the energy up-conversion effect of Er^{3+} ions and thermal damage of waveguides [20,21], which are bottlenecks limiting the application of EDWAs.

Organic complexes were initially synthesized for efficient energy transfer between ligands and rare-earth ions. Organic ligands have continuous absorption bands and large absorption cross sections (10^{-22} – 10^{-23} m^2) [22,23] in the UV wave band. The ultraviolet and visible energies absorbed by organic ligands can be effectively transferred to the excited-state energy level of the central rare earth ions. The energy transfer efficiency can reach five times that between rare-earth ions, such as Yb^{3+} and Er^{3+} ions [24]. However, the advantages of organic complexes have not been completely utilized, owing to the limitations of the traditional research methods of the optical fiber amplifiers and inorganic waveguide amplifiers. They are only used to solve the problem of the low solubility of rare earth ions in polymer hosts in the research field of optical waveguide amplifiers.

Based on this fact, complex $\text{Er}(\text{TMHD})_3$ (TMHD:2,2,6,6-tetramethyl-3,5-heptanedione)-doped PMMA was prepared as the active material to fabricate polymer waveguides with three different structures using standard photolithography and inductively coupled plasma (ICP) technology. The absorption and photoluminescence (PL) spectra were recorded. Optical gains were demonstrated by the intramolecular energy transfer effect between the organic ligand TMHD and Er^{3+} ions. Under the vertical top pumping of 365 and 405 nm light emitting diodes (LEDs), the relative gains of 3.5 and 4.1 dB cm^{-1} at 1.55 μm were obtained, respectively, in 1-cm-long rectangular waveguides with $\text{Er}(\text{TMHD})_3$ -doped PMMA as an active core. A maximum relative optical gain of 3.0 dB cm^{-1} was achieved in waveguides based on evanescent-field coupling with passive SU-8 as channel waveguides and $\text{Er}(\text{TMHD})_3$ -doped PMMA as the upper cladding. An aluminum (Al) reflector with $\text{Er}(\text{TMHD})_3$ -doped PMMA as a lower cladding was added to evanescent-field waveguides to improve the absorption efficiency of the LED and gain performance. The relative gain doubled and improved to 6.7 dB cm^{-1} because of the stimulated excitation in both the lower and upper claddings.

The propagation loss and coupling loss of three different waveguides at 1.55 μm were evaluated using the cut-back method. The sensitization mechanism between the organic ligand TMHD and Er^{3+} ions is discussed. This result demonstrates the possibility of optical amplification of the Er^{III} complex through an intramolecular energy transfer effect with low-power LED pumping. $\text{Er}(\text{TMHD})_3$ -doped PMMA and its proper LED pumping technology could undoubtedly greatly reduce the commercial cost of EDWA in planar photonic integration.

2. Experiment and analysis

2.1. Synthesis of complex $\text{Er}(\text{TMHD})_3$ -doped PMMA polymer

$\text{Er}(\text{TMHD})_3$ (Erbium(III)-tris-(2,2,6,6-tetramethyl-3,5-heptanedione)) with a purity of > 99% was purchased from Sigma-Aldrich (Shanghai) Trading Co. Ltd. In general, a choosing the ligand is crucial for proficient ligand-to-central ion energy transfer, which requires desirable matching of the emissive energy level of Ln^{3+} and the ligand excited state. The organic ligand TMHD, a β -diketone ligand, is desirable for sensitizing lanthanide emissions, as it possesses a strong π - π^* absorption within a large wavelength range in the ultraviolet region. It acts as an “antenna” to transfer the energy of π - π^* absorption to effectively illuminate levels of central ions and can form brightly emissive and thermally improved adducts with lanthanide ions. It has

been used to improve the quantum efficiency, solubility, and color purity of high-performance electroluminescent materials [25–29]. The singlet S_1 and triplet T_1 excited states of TMHD match the ${}^4F_{7/2}$ energy level of the Er^{3+} ions. Hence, the energy absorbed by the ligand can be directly transferred to the Er^{3+} ions. PMMA is a polymer with excellent optical properties and has the advantages of high transmittance, flexibility, and easy processing [30]. Therefore, it was chosen as the polymer host in this study. $Er(TMHD)_3$ complex (0.01 g) was dissolved in 0.2 mL toluene and subsequently added to a solution of 1 g PMMA (Macklin Biochemical Co. Ltd.) in 4 mL *n*-butyl acetate. Subsequently, the mixture was put in a glass weighing bottle and stirred at room temperature for 48 h, then heated in a vacuum oven for 6 h with a gradient heating process from 75 to 120 °C, to remove solvent and form an approximately 180- μ m-thick transparent film. The doping concentration of $Er(TMHD)_3$ in PMMA was 1 wt%, and the concentration of Er^{3+} ions was approximately 4.4×10^{25} ions/m³. In order to produce several decibels of optical gain in a centimeter-long waveguide, the doping concentration of Er^{3+} ions in polymer hosts should as high as possible. However, high concentration easily leads to poor film-formation and concentration quenching, thus increase the transmission loss and scattering loss of the waveguide, which is an unfavorable factor for optical gain. On the premise of ensuring the film with lower surface roughness, the concentration of ~ 1.0 wt% for $Er(TMHD)_3$ in PMMA is almost the maximum doping concentration. Additionally, inorganic $ErCl_3 \cdot 6H_2O$ powder and $ErCl_3 \cdot 6H_2O$ -doped PMMA film were prepared to compare the absorption properties of the complexes.

2.2. Absorption and photoluminescence properties

The absorption spectra of $Er(TMHD)_3$ powder and $Er(TMHD)_3$ -doped PMMA film were recorded using a Shimadzu UV-Vis-NIR spectrophotometer at room temperature, as shown in Fig. 1. The $Er(TMHD)_3$ and $ErCl_3 \cdot 6H_2O$ powders exhibited several absorption peaks at 365, 375, 405, 450, 488, 522, 544, 654, 795, and 978 nm, corresponding to the intrinsic transitions of Er^{3+} ions from the ground state ${}^4I_{15/2}$ to the ${}^4G_{9/2}$, ${}^4G_{11/2}$, ${}^2H_{9/2}$, ${}^4F_{5/2}$, ${}^4F_{7/2}$, ${}^2H_{11/2}$, ${}^4S_{3/2}$, ${}^4F_{9/2}$, ${}^4I_{9/2}$, and ${}^4I_{11/2}$ excited states, respectively [31]. Compared to the absorption of $ErCl_3 \cdot 6H_2O$ in the UV band, the $Er(TMHD)_3$ powder showed a significant continuous absorption band in the wavelength range of 300–350 nm, which is attributed to the absorption of the TMHD ligand [32]. Compared with the $Er(TMHD)_3$ powder, the absorption intensity of almost all the intrinsic absorption peaks of Er^{3+} ions is attenuated in the $Er(TMHD)_3$ -doped PMMA film because the concentration of Er^{3+} ions in the polymer film is much lower than that in the powder. However, there is still a strong absorption in the ultraviolet band from 300 to 350 nm, which mainly depends on the absorption of the TMHD and PMMA ligands. The pump rate R_p is an important factor affecting the optical gain performance of the waveguide amplifier, which can be determined by the absorption intensity σ_{abs} multiplied by the photon flux density φ : $R_p = \sigma_{abs} \times \varphi$ [33]. Meanwhile, the photon flux density φ is determined by the pump power per unit area. Therefore, a large absorption intensity σ_{abs} can improve the pump rate R_p . For the traditional pumping method using semiconductor lasers to achieve the intrinsic absorption of Er^{3+} ions at 1480 or 980 nm, a relatively large absorption intensity σ_{abs} can be obtained by increasing the doping concentration of Er^{3+} ions or co-doping Yb^{3+} ions in the material. However, it is easy to cause a concentration quenching and up-conversion effect [34,35], which is not conducive to the down-conversion emission of Er^{3+} ions at 1.53 μ m. A high photon flux density φ requires high laser energy, causing destructive thermal damage to the waveguide end face.

In this study, a new approach that is different from the traditional research idea was proposed, which was based on the intramolecular energy transfer mechanism between the ligand TMHD and central Er^{3+} ions in the UV band. Moreover, the intrinsic absorption of Er^{3+} ions at 365, 375, and 405 nm, corresponding to the ${}^4G_{9/2}$, ${}^4G_{11/2}$, and ${}^2H_{9/2}$ energy levels, respectively, were also utilized. Depending on the large absorption intensity σ_{abs} of approximately 6.1×10^{-23} m²

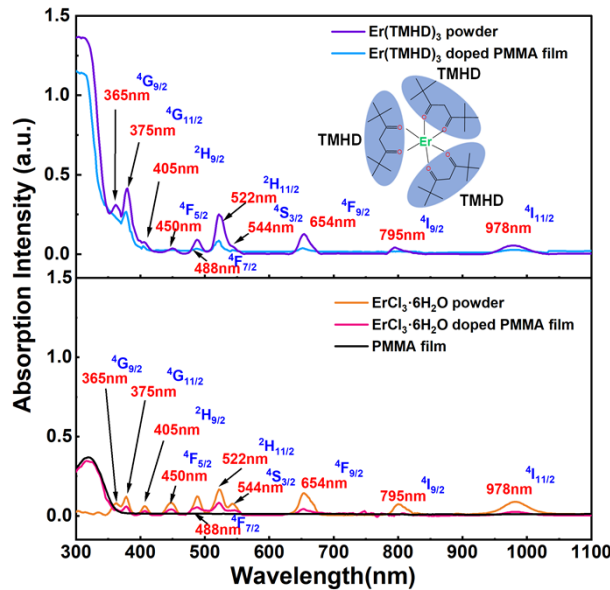


Fig. 1. Absorption spectra of $\text{Er}(\text{TMHD})_3$ and $\text{ErCl}_3 \cdot 6\text{H}_2\text{O}$ powder and doped PMMA films.

at 300–400 nm in $\text{Er}(\text{TMHD})_3$ -doped PMMA, a higher pumping rate R_p can be provided and the waveguide fabricated with $\text{Er}(\text{TMHD})_3$ -doped PMMA is expected to achieve optical gain under excitation of low-power UV LEDs. This method can reduce the influence of concentration quenching and avoid destructive thermal damage to the waveguide pumped by a high-power laser.

Figure 2 presents the photoluminescence (PL) spectra of the $\text{Er}(\text{TMHD})_3$ -doped PMMA film excited by 365 and 405 nm LEDs under the same 130 mW pump power, respectively. The irradiation spectra of 365 and 405 nm LEDs cover 320–400 nm and 370–420 nm, respectively. The PL peak at 1535 nm is due to the transition of Er^{3+} ions from the excited state $^4\text{I}_{13/2}$ to the ground state $^4\text{I}_{15/2}$ [36]. The fluorescence full width at half maximum (FWHM) of 365 and 405 nm are both approximately 52 nm. Compared with the FWHM value of Er^{3+} ions in inorganic hosts [37], the broadening of the emission is associated to the coupling of f–f electronic transition of Er^{3+} ions with vibrational modes of the PMMA matrix [38]. Since the absorption intensity of $\text{Er}(\text{TMHD})_3$ -doped PMMA at 365 nm is higher than that at 405 nm, the film excited by the former has stronger PL intensity, indicating that better gain performance can be obtained by using a 365 nm LED excitation. The PL intensity linearly increases with increasing pump power, as shown in Fig. 2(b).

2.3. Waveguide fabrication

The doping concentration of Er^{3+} ions in the polymer host should reach 10^{25} – 10^{26} ions/ m^3 [39,40], which is approximately two orders of magnitude higher than that in EDFA, to produce an optical gain of several decibels in a centimeter-long waveguide. Such a high doping concentration leads to poor uniformity, poor solubility, and high propagation loss. Therefore, one of the key factors in preparing high-performance EDWA is obtaining polymer films with good film-forming qualities. Figure 4(a) displays an atomic force microscope (AFM) micrograph of the $\text{Er}(\text{TMHD})_3$ -doped PMMA film. The root-mean-square roughness R_q was 0.35 nm for the 6- μm -thick film on the Si substrate after thermal annealing. Compared with $\text{LaF}_3:\text{Er}^{3+}, \text{Yb}^{3+}$ nanocrystal-doped organic-inorganic hybrid materials [41] and $\text{NaYF}_4/\text{NaLuF}_4:\text{Yb}, \text{Er}$ nanocomposite-doped PMMA

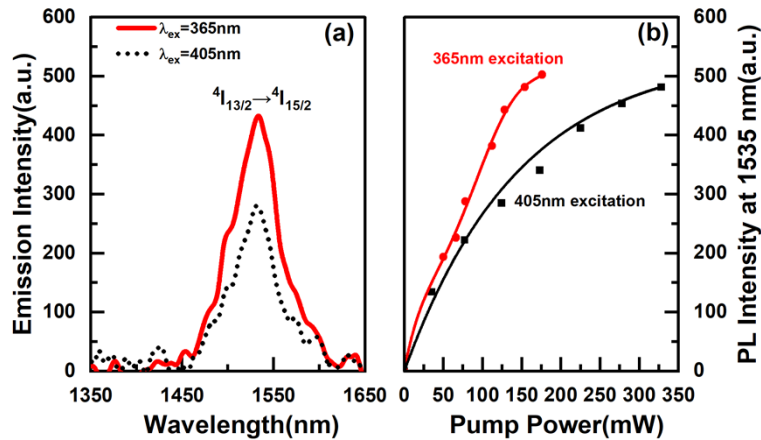


Fig. 2. Room temperature infrared PL spectra of the Er(TMHD)₃-doped PMMA film. (a) Under the excitation of 365 nm and 405 nm LEDs (130 mW), respectively. (b) PL intensity at 1535 nm as a function of the LED pump power.

[42], Er(TMHD)₃-doped PMMA has better film quality, which is conducive to obtaining a lower transmission loss of the optical signal.

Three waveguide structures were designed and fabricated using Er(TMHD)₃-doped PMMA as the active material to compare their optical gain performance. Their cross sections are shown in Fig. 3. For the rectangular waveguide in Fig. 3(a), Er(TMHD)₃-doped PMMA polymer with a thickness of 4 μm was spin-coated as the core layer on a silicon substrate with 2-μm-thick SiO₂ as the lower cladding. The refractive index of the core was 1.483 at 1550 nm wavelength. Then, an aluminum film of 50 nm thickness was deposited onto the core layer surface to form a dry etching mask by magnetron sputtering. A group of rectangular waveguides with a cross-section of 4 × 4 μm² was fabricated using standard photolithography and inductively coupled plasma (ICP) etching. The scanning electron microscope (SEM) micrographs (SUPRA 55 SAPPHIRE) of the rectangular waveguides is shown in Fig. 4(b). Figure 3(b) displays the cross-section of the evanescent-field waveguides with passive SU-8 polymer as channel waveguides on a silicon substrate with a 2-μm-thick SiO₂ as the lower cladding and a ~1-μm-thick Er(TMHD)₃-doped PMMA as the upper cladding. The refractive index of SU-8 was 1.552 at 1550 nm. When the optical signal laser travels in the passive SU-8 channel waveguides, the photon energy can enter from the passive core to the active upper cladding in the form of an evanescent wave, triggering stimulated radiation of the active material in the upper cladding under the excitation of the pump source. A SEM micrograph of the evanescent-field waveguides is shown in Fig. 4(c). A 100-nm-thick Al mirror was first sputtered on the SiO₂ layer and then spin-coated with a 6-μm-thick Er(TMHD)₃-doped PMMA as the lower cladding to improve the utilization efficiency of the radiation of the LED. Then, SU-8 channel waveguides were fabricated and coated with Er(TMHD)₃-doped PMMA as the upper cladding. Er³⁺ ions contained in the lower cladding could help increase the number of particles participating in the stimulated radiation, which is expected to further improve the gain performance. The cross-section of the waveguides and the propagation path of the evanescent wave are presented in Figs. 3(c) and (d). A SEM micrograph of the evanescent-field waveguides with an Al mirror is shown in Fig. 4(d).

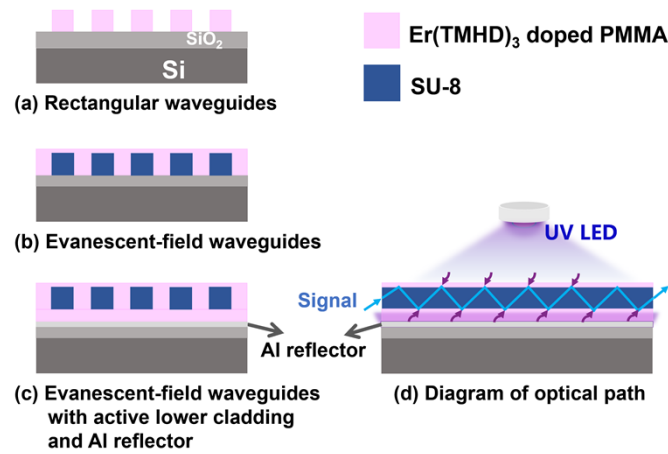


Fig. 3. Schematic diagram of the three structures of waveguides. (a) Rectangular waveguides with Er(TMHD)₃-doped PMMA as channel waveguides. (b) Evanescent-field waveguides with SU-8 polymer as channel waveguides and Er(TMHD)₃-doped PMMA as upper cladding. (c) Evanescent-field waveguides with Er(TMHD)₃-doped PMMA as active cladding and an Al reflector.

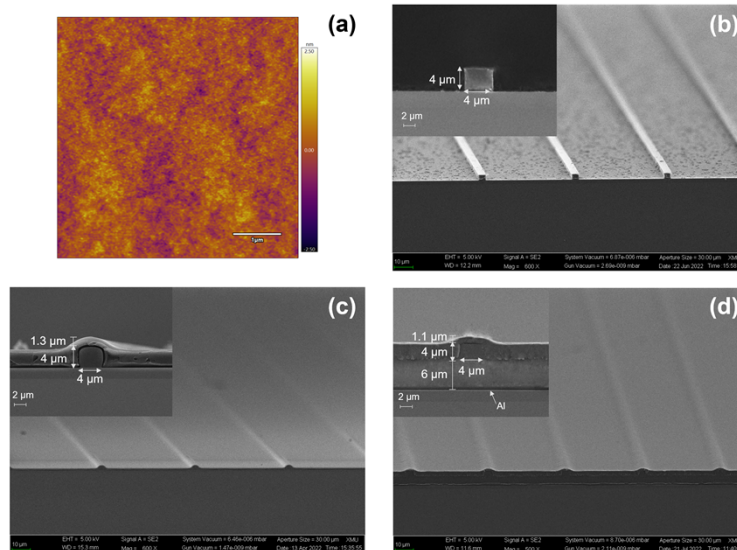


Fig. 4. (a) AFM micrograph of the Er(TMHD)₃-doped PMMA film. (b) Top view and cross-section (inset) SEM micrographs of active rectangular waveguides ($4 \times 4 \mu\text{m}^2$) with Er(TMHD)₃-doped PMMA as channel waveguides. (c) Top view and cross-section (inset) SEM micrographs of evanescent-field waveguides with SU-8 polymer as channel waveguides ($4 \times 4 \mu\text{m}^2$) and Er(TMHD)₃-doped PMMA as upper cladding ($\sim 1\text{-}\mu\text{m}$ -thick on top surface of the waveguide). (d) Top view and cross-section (inset) SEM micrographs of evanescent-field waveguides with Er(TMHD)₃-doped PMMA as active lower cladding ($6\text{-}\mu\text{m}$ -thick) and a 100-nm -thick Al reflector to improve the utilization efficiency of the radiation of the LED.

3. Results and discussion

An experimental setup for optical gain measurement was established by adopting the vertical top-pumping mode of the LED, as shown in Fig. 5. A 1550 nm laser source (KG-DFB-15-10-SM-FA, Yuwei, China) was used as the signal source, and two LEDs with different central wavelengths (Yonglin Optoelectronics Co., Ltd), such as 365 nm (YL-UVAHP-6565-365) and 405 nm (YL-UVAHP-6060-405), were used as the pump source. The LED was placed approximately 2 mm above the Er (TMHD)₃-doped PMMA waveguides. The viewing angle of the LED was 140°, and the total illumination area was approximately 1 cm², which almost completely covered the area of a 1-cm-long waveguide device. The power available on the device was approximately 295 mW based on the irradiation intensity distribution when the power of the LED was 328 mW. Therefore, the radiation efficiency of the LED power collected on the device in the total power of the LED were estimated to be approximately 90% [43]. The input signal laser was coupled to the optical waveguides using a single-mode fiber with an isolator. The output signal was coupled to an optical spectrometer (Ocean Optics FLAME-NIR-INTSMA25).

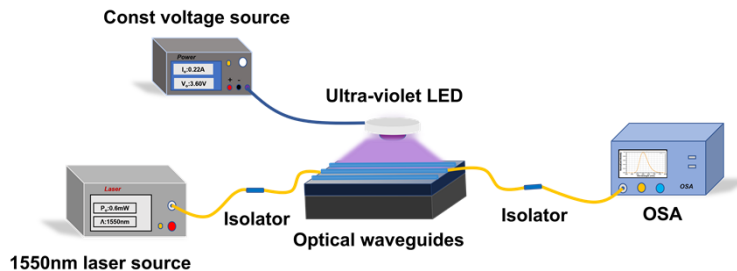


Fig. 5. Experimental setup for the optical gain of waveguides via the top-pumping LED mode.

The relative gain is defined as $10\lg(P_{P+S}/P_S)$ [44], where P_{P+S} and P_S are the output signal powers measured with and without pump power, respectively. Figure 6 shows the relationship between the output optical signal intensity and the pump power under excitation of 365 and 405 nm LEDs, respectively, in a 1-cm-long rectangular waveguide. The output signal intensity linearly increased as the pump power increased. The relative gains of rectangular waveguide could reach approximately 3.5 and 4.1 dB cm⁻¹ under the excitation of a 405 nm (328 mW) and 365 nm (176 mW), respectively, when the output power of the 1550 nm signal laser was 0.6 mW. Under the excitation of the 405 nm LED, the pump power required to achieve the same level of gain values of approximately 3.5 dB cm⁻¹ was almost twice that of the 365 nm LED; hence, the excitation effect of the 365 nm LED was better than that of the 405 nm LED, which is consistent with the conclusion obtained from the PL spectra. At a fixed pump power, a small-signal gain phenomenon was observed. The gain value slightly decreased as the optical power of the input signal increased. The maximum gain value decreased from 4.1 to 2.1 dB cm⁻¹ as the signal power varied from 0.6 to 0.8 mW with an excitation of the 176 mW 365 nm LED, and the gain variation trend was the same under the 405 nm excitation, as shown in the inset of Figs. 6(a) and (b).

Relative gains can also be obtained in waveguides based on evanescent-field coupling. The waveguide structure is presented in Fig. 3(b). Figure 7(a) shows the relationship between the output optical intensity and pump power under the excitation of different LEDs based on evanescent-field waveguides with Er(TMHD)₃-doped PMMA as the upper cladding. The maximum gains were 3.0 and 2.5 dB cm⁻¹ under the excitation of a 365 nm LED (176 mW) and a 405 nm LED (328 mW), respectively, when the output power of the signal power was 0.6 mW. Similar to the gain performance of the rectangular waveguide, the gain linearly increased with

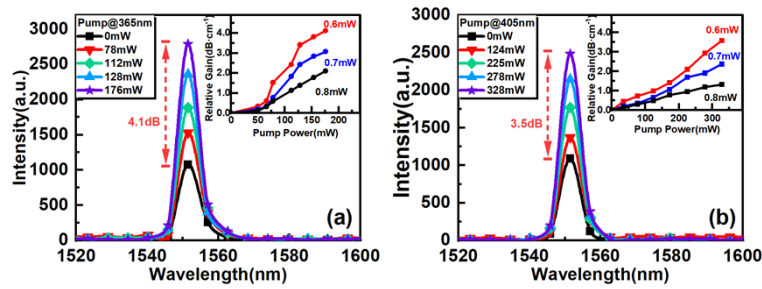


Fig. 6. (a), (b) Relationship between the output signal intensity and relative gain at 1.55 μm in rectangular waveguides with $\text{Er}(\text{TMHD})_3$ -doped PMMA as channel waveguides under excitation of 365 nm and 405 nm LEDs, respectively. The insets show the relationship between the relative gain and different signal power.

the pump power. The gain value reaches 6.9 dB (2.3 dB cm^{-1}) in a 3-cm-long evanescent-field waveguide under 365 nm LED excitation, as shown in the inset of Fig. 7(a). The longer the waveguide (1–3 cm), the higher the optical gain (3–6.9 dB), but the smaller the gain obtained in the waveguide per unit length (3– 2.3 dB cm^{-1}), which is not a fixed value. The total relative gain increases because the amount of Er^{3+} ions increases with increasing waveguide length. However, the light emitted by one LED cannot completely cover the entire long straight waveguide; therefore, Er^{3+} ions are not entirely activated. We consider this is one of the reasons for the reduction in gain per unit length. Based on the data shown in Fig. 7(b), the relative gain performance of 365 nm LED pumping is still better than that of 405 nm LED pumping. When the power of signal laser changes from 0.6 to 0.7 mW, the gain also changes from 3.0 and 2.5 dB cm^{-1} to 2.3 and 2.1 dB cm^{-1} , respectively, under the excitation of a 365 nm LED (176 mW) and a 405 nm LED (328 mW). Similar to the trend of the rectangular waveguide, the gain value slightly decreased as the input signal optical power increased.

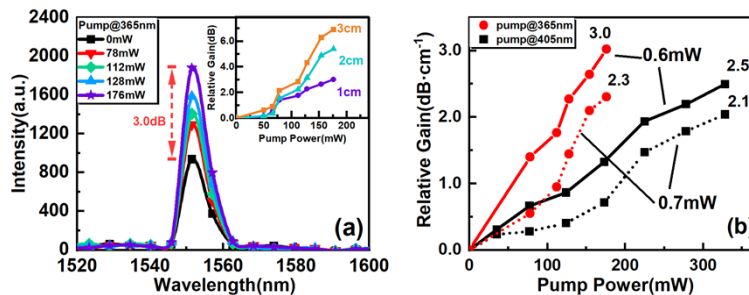


Fig. 7. (a) Relationship between the output signal intensity in evanescent-field waveguide with $\text{Er}(\text{TMHD})_3$ -doped PMMA as upper cladding. The inset shows the gain in evanescent-field waveguides of different lengths. (b) Comparison of relative gains obtained in evanescent-field waveguides with different signal power under 365 and 405 nm LED excitations.

$\text{Er}(\text{TMHD})_3$ -doped PMMA was added as an active lower cladding and an aluminum reflector was grown under the lower cladding to improve the gain performance of evanescent-field waveguides. The waveguide structure of evanescent-field waveguides with active lower cladding and an Al reflector is shown in Figs. 3(c) and (d). The pump light can penetrate the waveguide and reflect back to the active upper and lower cladding through the Al reflector when the LED vertically radiates the waveguide from the upper surface at a distance of 2 mm, and then excite the active materials in the cladding. Due to the presence of stimulated excitation in both the

upper and lower cladding, with the improved pump efficiency, relative gains of 6.7 and 5.2 dB cm⁻¹ at 1550 nm are observed in a 1-cm-long waveguide under 365 nm (176 mW) and 405 nm (328 mW) LEDs (328 mW) pumping, respectively, as shown in Figs. 8(a) and (b). In contrast to 3.0 and 2.5 dB cm⁻¹ of evanescent-field waveguides, the maximum relative gains of 6.7 and 5.2 dB cm⁻¹ are more than doubled and exceed the gain values of 4.1 and 3.5 dB cm⁻¹ of the rectangular waveguides, under 365 nm (176 mW) and 405 nm LEDs (328 mW) pumping, respectively, as shown in Figs. 8(c) and (d). Otherwise, as shown in the inset of Figs. 8(a) and (b), the maximum gains increased from 6.7 and 5.2 dB to 9.6 and 7.6 dB when the length of waveguide varied from 1 to 2 cm; but the gain per unit length decreased from 6.7 and 5.2 dB cm⁻¹ to 4.8 and 3.8 dB cm⁻¹, under 365 nm (176 mW) and 405 nm LEDs (328 mW) pumping, respectively, which is the same trend as that of the evanescent-field waveguide. Another way to improve the gain per unit length is to use the LED array in vertical top pumping technology such that the entire long straight waveguide can be completely irradiated by LEDs. Alternatively, curved spiral waveguides can be prepared and better covered in the LED irradiation range to obtain higher gain per unit length. In addition, due to the weak absorption of complex Er(TMHD)₃ at 978 nm, it is difficult to obtain the luminescence of Er³⁺ ions at 1550 nm in these three waveguide structures under excitation of a conventional 976 nm semiconductor laser.

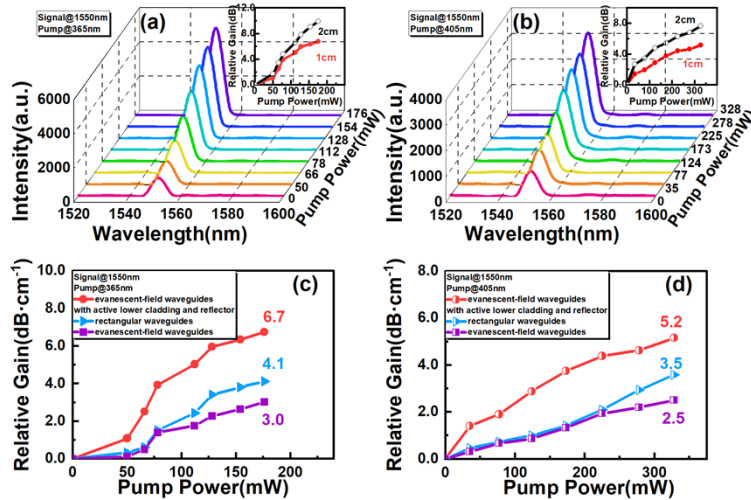


Fig. 8. (a), (b) Relationship between the output signal intensity in evanescent-field waveguide with active cladding and Al reflector. The insets show the relative gain of waveguide with different lengths. (c), (d) Comparison of relative gains as a function of pump power in three different structures of the waveguide.

The relationship between the relative gain $G(L)_{rel}$, internal gain $G(L)_{int}$, and net gain $G(L)_{net}$ can be described by Eqs. (1) and (2) [45].

$$G(L)_{rel} = G(L)_{int} + \alpha_{loss}, \quad (1)$$

$$G(L)_{int} = G(L)_{net} + \alpha_{cou}, \quad (2)$$

where α_{loss} is the propagation loss of the waveguide and α_{cou} is the coupling loss of the two end facets of the waveguide. Using the cut-back method, the propagation and coupling losses of three different waveguides at 1550 nm were measured, as shown in Fig. 9(a). The coupling loss is approximately 2.0 dB/facet. Compared with the propagation loss of 3.5 dB cm⁻¹ in the active rectangular waveguide, the propagation loss of the evanescent-field waveguide using

passive SU-8 as the core and Er(TMHD)₃-doped PMMA as the upper cladding is approximately 1.8 dB cm⁻¹. For the evanescent-field waveguide with an Al reflector, the propagation loss was approximately 1.7 dB cm⁻¹. The propagation loss of the active waveguide is higher than that of the passive waveguide because of the increase in the absorption loss and scattering loss with doped active materials, as well as the roughness of the active rectangular waveguide. According to the above formula, the gain results are displayed in Figs. 9(b), (c), and (d). Under the excitation of 365 nm LED, the maximum gain $G(L)_{rel}$, $G(L)_{int}$, and $G(L)_{net}$ in the rectangular waveguide are 4.1, 0.6, and -3.4 dB cm⁻¹. Meanwhile, $G(L)_{rel}$, $G(L)_{int}$, and $G(L)_{net}$ in the evanescent-field waveguide are 3.0, 1.2, and -2.8 dB cm⁻¹, respectively. A negative net gain indicates that the optical loss is greater than the gain generated in the waveguide. The higher internal gain and net gain of the evanescent-field waveguide than that of the rectangular waveguide are due to the low propagation loss of the passive waveguide. For the evanescent-field waveguide with an Al reflector, the overall evaluation of gain is the best among the three waveguide structures. The maximum gain value of $G(L)_{rel}$, $G(L)_{int}$, and $G(L)_{net}$ are 6.7, 5.0, and 1.0 dB cm⁻¹, respectively. As a comparison, under excitation of the 405 nm LED, the maximum net gain $G(L)_{net}$ in the rectangular waveguide, evanescent-field waveguide, and evanescent-field waveguide with the Al reflector are -4.0, -3.3, and -0.5 dB cm⁻¹, respectively.

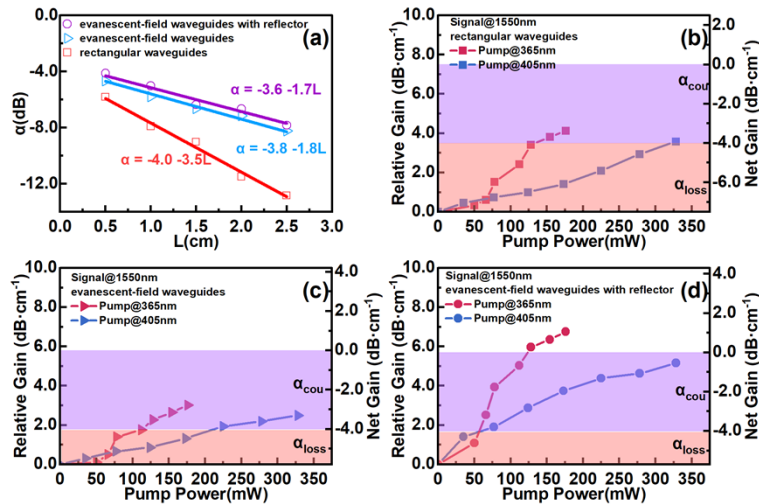
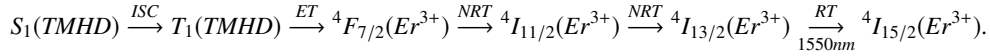


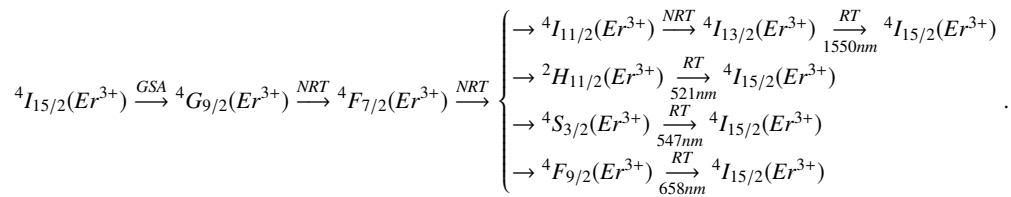
Fig. 9. (a) Measured propagation loss and coupling loss of different waveguides at 1550 nm by cut-back method. Gains of (b) rectangular waveguide, (c) evanescent-field waveguide, and (d) evanescent-field waveguide with an Al reflector. (The red part is the propagation loss α_{loss} , and the purple part is the coupling loss α_{cou} .)

Based on the absorption and PL spectra and the gain measurement results of the waveguides, a ligand-sensitization scheme between the organic ligand TMHD and Er³⁺ ions under the excitation of the UV LEDs is presented in Fig. 10. It is generally assumed that the major energy transfer mechanism between an excited state on an organic molecule and a lanthanide ion is via the triplet state of the organic molecule; thus, photoexcited molecules must undergo intersystem crossing (ISC) [46]. The energy level of the triplet excited state (T_1 , 22200 cm⁻¹) of ligand TMHD matches that of the $^4F_{7/2}$ state (20400 cm⁻¹) of Er³⁺ ions with an energy gap of 1800 cm⁻¹, which can inhibit reverse energy transfer and promote efficient energy transfer without additional high-energy phonon assistance. The quantum number difference ΔJ of the total angular momentum of the excited state $^4F_{7/2}$ and ground state $^4I_{15/2}$ is 4, satisfying the Förster resonance energy transfer (FRET) mechanism [47–49]. Therefore, under the excitation

of UV LEDs, the ligand TMHD can obtain energy and transfer from the ground state S_0 to the first excited state S_1 , and then realize energy transfer from the S_1 to T_1 state via the ISC process, followed by energy transfer from the T_1 state of TMHD to the ${}^4F_{7/2}$ state of Er^{3+} ions. Finally, Er^{3+} ions complete two non-radiative transition (NRT) processes from the ${}^4F_{7/2}$ to ${}^4I_{11/2}$ state and from the ${}^4I_{11/2}$ to ${}^4I_{13/2}$ state, and a radiative transition (RT) process from ${}^4I_{13/2}$ to ${}^4I_{15/2}$, and finally realize photon emission at 1550 nm. The energy transfer path is summarized in route 1:



Er^{3+} ions in the ground state ${}^4I_{15/2}$ can also be excited to ${}^4G_{9/2}$, ${}^4G_{11/2}$, and ${}^2H_{9/2}$ by ground state absorption (GSA) under the excitation of UV LEDs, and then through the NRT process to the ${}^4F_{7/2}$ state. On the one hand, Er^{3+} ions in the ${}^4F_{7/2}$ state can achieve 1550 nm luminescence via the two aforementioned NRT processes and one RT process via route 1 [50]. On the other hand, the Er^{3+} ions in the ${}^4F_{7/2}$ state can transition to the ${}^2H_{11/2}$, ${}^4S_{3/2}$, and ${}^4F_{9/2}$ states, respectively, in the NRT process [51], from where they radiatively decay to the ground state ${}^4I_{15/2}$, realizing green and red emissions at 521, 547, and 658 nm, respectively, which is consistent with the PL spectrum of the $Er(TMHD)_3$ -doped PMMA film in the visible light bands with the excitation of a 365 nm LED, as shown in Fig. 10(c). The energy-level transition processes of Er^{3+} ions excited by UV LEDs are summarized as follows:



Note that the three visible light emissions obtained here should also be considered as down-conversion, which has the same properties as the down-conversion luminescence of Er^{3+} ions at a wavelength of 1550 nm. This is because Er^{3+} ions in the ground state almost transit to the highest energy level via the GSA process with ultraviolet energy, and the pump energy is transferred from the higher excited states of Er^{3+} ions to the lower excited states. However, for the current mainstream pumping technology with a 980 nm laser as the pump source in the research of EDWAs, Er^{3+} ions are excited from the ${}^4I_{15/2}$ to ${}^4I_{11/2}$ state via the GSA process and then excited to the ${}^4F_{7/2}$ state via excited state absorption (ESA) or cross-relaxation (CR) processes from neighboring Er^{3+} ions, as shown in Fig. 10(b). The Er^{3+} ions in the ${}^4F_{7/2}$ state can transit to the ${}^2H_{11/2}$ and ${}^4S_{3/2}$ states via the NRT process and then transition from these two states to the ${}^4I_{15/2}$ state to generate two green emissions. Meanwhile, the excited Er^{3+} ions in the ${}^4I_{11/2}$ state can decay non-radiatively to the lower excited state ${}^4I_{13/2}$. They can be excited to the ${}^4F_{9/2}$ state via the ESA process with the excitation of a 980 nm laser, causing the red emission via the RT process [52]. Here, the green and red emissions are up-conversion luminescence, and the 980 nm pump energy is transferred from the lower excited states to the higher excited states.

Figure 11 presents the application prospects of $Er(TMHD)_3$ -doped PMMA as active materials to active two-stage amplification at a wavelength of 1.55 μm in planar photonic integration. The schematic diagram integrates a spiral waveguide and a 1×8 beam splitter [53]. $Er(TMHD)_3$ -doped PMMA was spin coated as the active upper cladding on passive waveguides. An Al reflector is added on the SiO_2 layer. Passive materials, such as polymer and SiO_2 , and $Er(TMHD)_3$ -doped PMMA active materials can be selected for the lower cladding as required. Thus, with only one LED pumping, the synchronous secondary amplification function of the whole chip with low power consumption, low optical loss, high efficiency, and easy integration can be realized based on the method of evanescent wave coupling combining with an Al reflector according to this study.

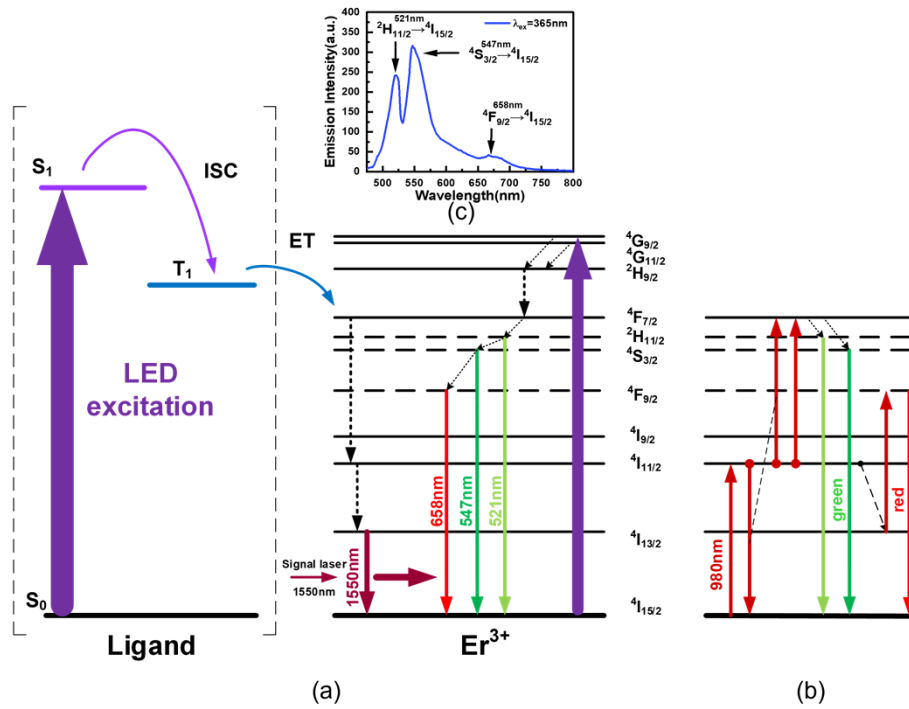


Fig. 10. (a) Intramolecular energy transfer mechanism of ligand- Er^{3+} ions and luminescence processes of Er^{3+} ions under a UV LED pumping. (b) Up-conversion luminescence at green and red lights under 980 nm LD pumping. (c) The visible emissions at 521, 547, 658 nm of the $\text{Er}(\text{TMHD})_3$ -doped PMMA film.

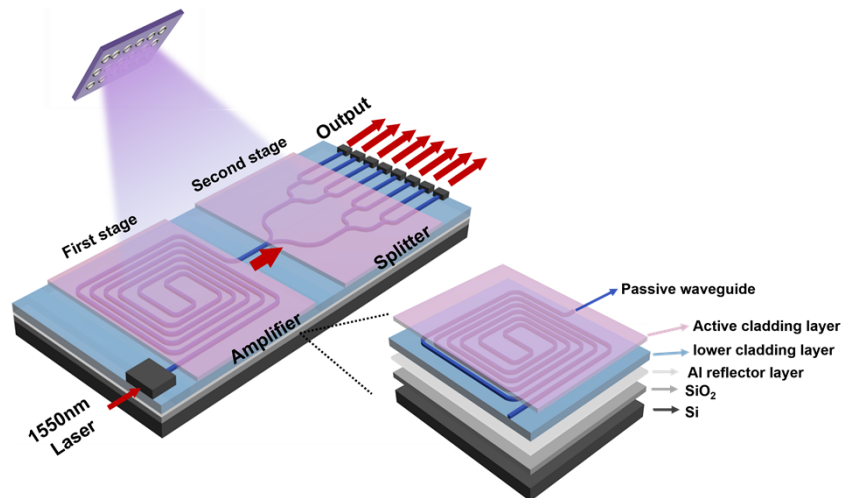


Fig. 11. Schematic diagram of the photonic integrated circuit based on this work.

4. Conclusions

Optical gains at a wavelength of 1.55 μm were demonstrated in polymer waveguide amplifiers based on complex $\text{Er}(\text{TMHD})_3$ -doped PMMA with the excitation of UV LEDs, instead of 980 nm lasers. The absorption and PL spectra were recorded. The absorption intensity of $\text{Er}(\text{TMHD})_3$ -doped PMMA at 365 nm is higher than that at 405 nm, causing the PL excited by the former to have a stronger intensity. Three different waveguide structures based on $\text{Er}(\text{TMHD})_3$ -doped PMMA polymer were fabricated. Under vertical top pumping of 365 nm (176 mW) and 405 nm LED (328 mW), the relative gains of 4.1 and 3.5 dB cm^{-1} at 1.55 μm were achieved in rectangular waveguide with cross-section of $4 \times 4 \mu\text{m}^2$, respectively. Based on evanescent-field coupling, the relative gain of 3.0 and 2.5 dB cm^{-1} were observed in a 1-cm-long evanescent-field waveguide under excitation of 365 and 405 nm LEDs respectively, when passive SU-8 was fabricated as channel waveguide and $\text{Er}(\text{TMHD})_3$ -doped PMMA as upper cladding. The optical gain was doubled and improved to 6.7 dB cm^{-1} under the excitation of a 176 mW 365 nm LED by adding $\text{Er}(\text{TMHD})_3$ -doped PMMA as the lower cladding and Al reflector in the evanescent-field waveguide because of the presence of stimulated excitation in both the upper and lower cladding and an improved absorption efficiency of the LED. The propagation loss and coupling loss of three different waveguides at 1.55 μm were evaluated using the cut-back method. The propagation loss of 3.5 dB cm^{-1} in rectangular waveguide with an active core was higher than that of 1.8 and 1.7 dB cm^{-1} in evanescent-field waveguide and evanescent-field waveguide with reflector with passive SU-8 core, respectively, because of the increase of absorption and scattering loss with doped active materials, as well as the roughness of the active rectangular waveguide. The sensitization mechanism between the organic ligand and Er^{3+} ions is also discussed.

These results indicate the possibility of optical amplification in EDWA based on $\text{Er}(\text{TMHD})_3$ complex-doped PMMA at 1.55 μm through the intramolecular energy transfer effect with low-power LED pumping. Optical loss can be compensated by conveniently integrating $\text{Er}(\text{TMHD})_3$ -doped PMMA into the waveguide parts of optical functional devices on various commercial photonic platforms.

Funding. National Key Research and Development Program of China (2021YFB2800500); National Natural Science Foundation of China (61875170, 61107023); Natural Science Foundation of Fujian Province (2022J01063).

Disclosures. The authors declare no conflict of interest.

Data availability. Data underlying the results presented in this paper are not publicly available at this time but may be obtained from the authors upon reasonable request.

References

1. H. C. Frankis, Y. R. Xie, R. J. Das, K. R. Chen, H. Rufenacht, G. Lamontagne, J. D. B. Bradley, and A. P. Knights, "Application of the TDFA window in true optical time delay systems," *Opt. Express* **30**(17), 30164–30175 (2022).
2. J. X. Zhou, Y. T. Liang, Z. X. Liu, W. Chu, H. S. Zhang, D. F. Yin, Z. W. Fang, R. B. Wu, J. H. Zhang, W. Chen, Z. Wang, Y. Zhou, M. Wang, and Y. Cheng, "On-chip integrated waveguide amplifiers on erbium-doped thin-film lithium niobate on insulator," *Laser Photonics Rev.* **15**(8), 2100030 (2021).
3. C. X. Wang, M. J. Zhang, Y. Z. Chen, Y. Wang, J. C. Lu, X. X. Huang, Y. H. Wei, L. Wan, S. Q. Huang, Z. Li, Z. Q. Chen, and Z. H. Li, "Synthesis and study of novel erbium-doped La_2O_3 - Al_2O_3 glasses for on-chip waveguide amplifier," *J. Alloys Compd.* **899**, 162915 (2022).
4. J. Ronn, J. H. Zhang, W. W. Zhang, Z. R. Tu, A. Matikainen, X. Leroux, E. Duran-Valdeiglesias, N. Vulliet, F. Boeuf, C. Alonso-Ramos, H. Lipsanen, L. Vivien, Z. P. Sun, and E. Cassan, "Erbium-doped hybrid waveguide amplifiers with net optical gain on a fully industrial 300 mm silicon nitride photonic platform," *Opt. Express* **28**(19), 27919–27926 (2020).
5. C. M. Naraine, J. W. Miller, H. C. Frankis, D. E. Hagan, P. Mascher, J. H. Schmid, P. Cheben, A. P. Knights, and J. D. B. Bradley, "Subwavelength grating metamaterial waveguides functionalized with tellurium oxide cladding," *Opt. Express* **28**(12), 18538–18547 (2020).
6. H. C. Frankis, H. M. Mbonde, D. B. Bonneville, C. L. Zhang, R. Mateman, A. Leinse, and J. D. B. Bradley, "Erbium-doped TeO_2 -coated Si_3N_4 waveguide amplifiers with 5 dB net gain," *Photonics Res.* **8**(2), 127–134 (2020).
7. W. Fan, B. Zhang, C. Wang, L. Ying, X. Yang, Z. Zhou, and D. Zhang, "Demonstration of optical gain at 1550 nm in an Er^{3+} - Yb^{3+} co-doped phosphate planar waveguide under commercial and convenient LED pumping," *Opt. Express* **29**(8), 11372–11385 (2021).

8. Q. Luo, C. Yang, Z. Z. Hao, R. Zhang, D. H. Zheng, F. Bo, Y. F. Kong, G. Q. Zhang, and J. J. Xu, "On-chip erbium-doped lithium niobate waveguide amplifiers [Invited]," *Chin. Opt. Lett.* **19**(6), 060008 (2021).
9. Z. X. Chen, Q. Xu, K. Zhang, W. H. Wong, D. L. Zhang, E. Y. B. Pun, and C. Wang, "Efficient erbium-doped thin-film lithium niobate waveguide amplifiers," *Opt. Lett.* **46**(5), 1161–1164 (2021).
10. Y. Liu, Z. R. Qiu, X. R. Ji, A. Lukashchuk, J. J. He, J. Riemensberger, M. Hafermann, R. N. Wang, J. Q. Liu, C. Ronning, and T. J. Kippenberg, "A photonic integrated circuit-based erbium-doped amplifier," *Science* **376**(6599), 1309–1313 (2022).
11. G. F. R. Chen, X. Zhao, Y. Sun, C. He, M. C. Tan, and D. T. H. Tan, "Low loss nanostructured polymers for chip-scale waveguide amplifiers," *Sci. Rep.* **7**(1), 3366 (2017).
12. Z. Q. Zhou, J. B. Xue, B. P. Zhang, C. Wang, X. C. Yang, W. Fan, L. Y. Ying, Z. W. Zheng, Y. J. Xie, Y. F. Wu, X. D. Yang, and D. Zhang, "Optical gain based on NaYF₄: Er³⁺, Yb³⁺ nanoparticles-doped polymer waveguide under convenient LED pumping," *Appl. Phys. Lett.* **118**(17), 173301 (2021).
13. Y. W. Fu, T. H. Sun, M. L. Zhang, X. C. Zhang, F. Wang, and D. M. Zhang, "Polymer/silica hybrid waveguide Y-branch power splitter with loss compensation based on NaYF₄:Er³⁺, Yb³⁺ nanocrystals," *Chin. Phys. B* **28**(10), 104206 (2019).
14. Y. L. Zhang, P. Lv, D. X. Wang, Z. K. Qin, F. Wang, D. M. Zhang, D. Zhao, G. S. Qin, and W. P. Qin, "KMnF₃:Yb³⁺,Er³⁺ core-active-shell nanoparticles with broadband down-shifting luminescence at 1.5 μm for polymer-based waveguide amplifiers," *Nanomaterials* **9**(3), 463 (2019).
15. T. H. Sun, Y. W. Fu, X. C. Zhang, J. M. Yan, F. Wang, and D. M. Zhang, "Gain enhancement of polymer waveguide amplifier based on NaYF₄:Er³⁺, Yb³⁺ nanocrystals using backward pump scheme," *Opt. Commun.* **488**, 126723 (2021).
16. C. Koeppen, S. Yamada, G. Jiang, A. F. Garito, and L. R. Dalton, "Rare-earth organic complexes for amplification in polymer optical fibers and waveguides," *J. Opt. Soc. Am. B* **14**(1), 155–162 (1997).
17. R. Sosa Fonseca, M. Flores, R. Rodriguez T, J. Hernández, and A. Muñoz F, "Evidence of Energy Transfer in Er³⁺-Doped PMMA-PAAc Copolymer Samples," *J. Lumin.* **93**(4), 327–332 (2001).
18. R. J. Curry and W. P. Gillin, "1.54 μm electroluminescence from erbium (III) tris(8-hydroxyquinoline) (ErQ)-based organic light-emitting diodes," *Appl. Phys. Lett.* **75**(10), 1380–1382 (1999).
19. O.-H. Park, S.-Y. Seo, B.-S. Bae, and J. H. Shin, "Indirect excitation of Er³⁺ in sol-gel hybrid films doped with an erbium complex," *Appl. Phys. Lett.* **82**(17), 2787–2789 (2003).
20. S. A. Vázquez-Córdova, M. Dijkstra, E. H. Bernhardt, F. Ay, K. Worhoff, J. L. Herek, S. M. Garcia-Blanco, and M. Pollnau, "Erbium-doped spiral amplifiers with 20 dB of net gain on silicon," *Opt. Express* **22**(21), 25993–26004 (2014).
21. W. R. Wang, G. L. Yu, S. N. Lai, and C. Jiang, "Facile approach towards the fabrication of compact and miniature Er³⁺-doped waveguide amplifiers," *OSA Continuum* **2**(5), 1773–1782 (2019).
22. X. Wang, K. Sun, L. J. Wang, X. J. Tian, Q. J. Zhang, and B. A. Chen, "Effect on the fluorescence branching ratio of different synergistic ligands in neodymium complex doped PMMA," *J. Non-Cryst. Solids* **358**(12-13), 1506–1510 (2012).
23. H. Zhan, J. Zhang, W. Fan, B. P. Zhang, L. Y. Ying, G. H. Xie, Z. S. Lin, H. S. Chen, H. Long, Z. M. Zheng, Z. W. Zheng, H. Xu, and D. Zhang, "Optical properties of organic neodymium complex doped optical waveguides based on the intramolecular energy transfer effect," *Opt. Mater. Express* **10**(10), 2624–2635 (2020).
24. D. Zhang, D. M. Zhang, X. Liang, F. Wang, and D. H. Guo, "A study of erbium-ytterbium-codoped polymer waveguide amplifier," *Microw. Opt. Technol. Lett.* **53**(9), 2157–2160 (2011).
25. G. Richards, J. Osterwyk, J. Flikkema, K. Cobb, M. Sullivan, and S. Swavey, "Monometallic and bimetallic europium(III) and terbium(III) complexes: Synthesis and luminescent properties," *Inorg. Chem. Commun.* **11**(11), 1385–1387 (2008).
26. J. Hwang, K. S. Yook, J. Y. Lee, and Y. H. Kim, "Synthesis and characterization of phenylpyridine derivative containing an imide functional group on an iridium (III) complex for solution-processable orange-phosphorescent organic light-emitting diodes," *Dyes Pigm.* **121**, 73–78 (2015).
27. Y. Kang, Y. L. Chang, J. S. Lu, S. B. Ko, Y. L. Rao, M. Varlan, Z. H. Lu, and S. N. Wang, "Highly efficient blue phosphorescent and electroluminescent Ir(III) compounds," *J. Mater. Chem. C* **1**(3), 441–450 (2013).
28. S. Y. Lee, S. E. Lee, Y. N. Oh, D. M. Shin, Y. K. Kim, and H. K. Kim, "Study of the characteristics of phosphorescent red organic light emitting diode using new iridium(III) complex with thiophene as dopant material," *Mol. Cryst. Liq. Cryst.* **659**(1), 108–114 (2017).
29. D. Singh, S. Bhagwan, A. Dalal, K. Nehra, R. K. Saini, K. Singh, A. P. Simantilleke, S. Kumar, and I. Singh, "Oxide ancillary ligand-based europium beta-diketonate complexes and their enhanced luminosity," *Rare Met.* **40**(10), 2873–2881 (2021).
30. G. L. Jimenez, C. Falcony, M. Szumera, P. Jelen, M. Lesniak, M. Kochanowicz, J. Zmojda, D. Dorosz, and P. Miluski, "Synthesis and characterization of poly(methyl methacrylate) co-doped with Tb(tmhd)₃ – Rhodamine b for luminescent optical fiber applications," *Spectrochim. Acta* **229**, 117893 (2020).
31. W. T. Carnall, P. R. Fields, and K. Rajnak, "Electronic energy levels in the trivalent lanthanide aquo ions. I. Pr³⁺, Nd³⁺, Pm³⁺, Sm³⁺, Dy³⁺, Ho³⁺, Er³⁺, and Tm³⁺," *J. Chem. Phys.* **49**(10), 4424–4442 (1968).
32. P. Miluski, M. Kochanowicz, J. Zmojda, T. Ragin, and D. Dorosz, "Spectroscopic investigation of Tb(tmhd)₃ – Eu(tmhd)₃ co-doped poly(methyl methacrylate) fibre," *Opt. Mater.* **87**, 112–116 (2019).

33. J. X. Hu, S. Karamshuk, J. Gorbaciova, H. Q. Ye, H. Lu, Y. P. Zhang, Y. X. Zheng, X. Liang, I. Hernandez, P. B. Wyatt, and W. P. Gillin, "High sensitization efficiency and energy transfer routes for population inversion at low pump intensity in Er organic complexes for IR amplification," *Sci. Rep.* **8**(1), 3226 (2018).
34. J. Rönn, L. Karvonen, C. Kauppinen, A. P. Perros, N. Peyghambarian, H. Lipsanen, A. Saynatjoki, and Z. P. Sun, "Atomic layer engineering of Er-ion distribution in highly doped Er:Al₂O₃ for photoluminescence enhancement," *ACS Photonics* **3**(11), 2040–2048 (2016).
35. L. Z. Hu, D. L. Sun, J. Q. Luo, H. L. Zhang, X. Y. Zhao, C. Quan, Z. Y. Han, K. P. Dong, M. J. Cheng, and S. T. Yin, "Effect of Er³⁺ concentration on spectral characteristic and 2.79 μm laser performance of Er:YSGG crystal," *J. Lumin.* **226**, 117502 (2020).
36. A. Q. Le Quang, E. Besson, R. Hierle, A. Mehdi, C. Reye, R. Corriu, and I. Ledoux-Rak, "Polymer-based materials for amplification in the telecommunication window: Influence of erbium complex concentration on relevant parameters for the elaboration of waveguide amplifiers around 1550 nm," *Opt. Mater.* **29**(8), 941–948 (2007).
37. K. Liu and E. Y. B. Pun, "Modeling and experiments of packaged Er³⁺-Yb³⁺ co-doped glass waveguide amplifiers," *Opt. Commun.* **273**(2), 413–420 (2007).
38. Y. Molard, C. Labbe, J. Cardin, and S. Cordier, "Sensitization of Er³⁺ infrared Photoluminescence Embedded in a Hybrid organic-inorganic Copolymer containing Octahedral Molybdenum Clusters," *Adv. Funct. Mater.* **23**, 4821–4825 (2013).
39. X. Liu, M. L. Zhang, and G. J. Hu, "Gain enhancement of the optical waveguide amplifier based on NaYF₄/NaLuF₄:Yb, Er NPs-PMMA integrated with a Si₃N₄ slot," *Nanomaterials* **12**(17), 2937 (2022).
40. Y. W. Fu, Y. Yang, T. H. Sun, Y. Tang, J. Li, H. Cui, W. P. Qin, F. Wang, G. S. Qin, and D. Zhao, "Polymer-based S-band waveguide amplifier using NaYF₄:Yb,Tm-PMMA nanocomposite as gain medium," *Opt. Lett.* **47**(1), 154–157 (2022).
41. Z. Chen, C. Y. Tian, S. H. Bo, X. H. Liu, and Z. Zhen, "Synthesis and the luminescent properties of the Nd³⁺ ions doped three kinds of fluoride nanocrystals in organic solvents," *Opt. Mater.* **48**, 86–91 (2015).
42. Y. Yang, F. Wang, S. T. Ma, M. Zhou, Y. B. Lang, G. S. Qin, D. M. Zhang, W. P. Qin, D. Zhao, and X. Zhang, "Great enhancement of relative gain in polymer waveguide amplifier using NaYF₄/NaLuF₄:Yb,Er-PMMA nanocomposite as gain media," *Polymer* **188**, 122104 (2020).
43. C. Wang, X. Liu, B. P. Zhang, G. H. Xie, Z. Q. Zhou, X. C. Yang, L. Y. Ying, Y. Mei, W. Fan, Z. S. Lin, Z. W. Zheng, and D. Zhang, "Optical Gain at 637 nm Wavelength in Polymer Waveguide Amplifier Under Commercial LED Pumping for Planar Photonic Integration," *Adv. Opt. Mater.* **10**(13), 2200205 (2022).
44. W. H. Wong, K. S. Chan, and E. Y. B. Pun, "Ultraviolet direct printing of rare-earth-doped polymer waveguide amplifiers," *Appl. Phys. Lett.* **87**(1), 011103 (2005).
45. D. L. Zhang, P. R. Hua, and E. Y. B. Pun, "Correct determination of net gain in Er-doped optical waveguide amplifier from pump-on/off measurement," *Opt. Commun.* **279**(1), 64–67 (2007).
46. J. G. Bünzli and S. V. Eliseeva, *Basics of Lanthanide Photophysics* (Springer, 2010).
47. O. L. Malta, "Ligand-rare-earth ion energy transfer in coordination compounds. A theoretical approach," *J. Lumin.* **71**(3), 229–236 (1997).
48. F. R. G. e Silva and O. L. Malta, "Calculation of the ligand-lanthanide ion energy transfer rate in coordination compounds: Contributions of exchange interactions," *J. Alloys Compd.* **250**(1-2), 427–430 (1997).
49. O. L. Malta and F. R. Gonçalves e Silva, "A theoretical approach to intramolecular energy transfer and emission quantum yields in coordination compounds of rare earth ions," *Spectrochim. Acta, Part A* **54**(11), 1593–1599 (1998).
50. H. F. Li, X. Q. Liu, C. Lyu, J. Gorbaciova, L. L. Wen, G. G. Shan, P. B. Wyatt, H. Q. Ye, and W. P. Gillin, "Enhanced 1.54-μm photo- and electroluminescence based on a perfluorinated Er(III) complex utilizing an iridium(III) complex as a sensitizer," *Light: Sci. Appl.* **9**(1), 32 (2020).
51. T. H. Sun, Y. W. Fu, Z. G. Cao, S. L. Tao, J. M. Yan, D. Zhao, D. Zhang, F. Wang, and D. M. Zhang, "Polymer/silica hybrid waveguide amplifier at 532 nm based on NaYF₄:Er³⁺, Yb³⁺ nanocrystals," *Opt. Lett.* **46**(21), 5385–5388 (2021).
52. D. Zhang, C. Chen, F. Wang, and D. M. Zhang, "Optical gain and upconversion luminescence in LaF₃: Er, Yb nanoparticles-doped organic-inorganic hybrid materials waveguide amplifier," *Appl. Phys. B* **98**(4), 791–795 (2010).
53. J. F. Mu, M. Dijkstra, J. Kortarik, H. Offerhaus, and S. M. Garcia-Blanco, "High-gain waveguide amplifiers in Si₃N₄ technology via double-layer monolithic integration," *Photonics Res.* **8**(10), 1634–1641 (2020).